

MagicTailor: Component-Controllable Personalization in Text-to-Image Diffusion Models

Donghao Zhou^{1*}, Jiancheng Huang^{2*}, Jinbin Bai³, Jiaze Wang¹, Hao Chen¹,
Guangyong Chen⁴, Xiaowei Hu^{5†}, Pheng-Ann Heng¹

¹CUHK ²SIAT, CAS ³NUS ⁴Zhejiang Lab ⁵Shanghai AI Lab

dhzhou@link.cuhk.edu.hk, huxiaowei@pjlab.org.cn

<https://correr-zhou.github.io/MagicTailor>

Abstract

Text-to-image diffusion models can generate high-quality images but lack fine-grained control of visual concepts, limiting their creativity. Thus, we introduce **component-controllable personalization**, a new task that enables users to customize and reconfigure individual components within concepts. This task faces two challenges: *semantic pollution*, where undesired elements disrupt the target concept, and *semantic imbalance*, which causes disproportionate learning of the target concept and component. To address these, we design **MagicTailor**, a framework that uses *Dynamic Masked Degradation* to adaptively perturb unwanted visual semantics and *Dual-Stream Balancing* for more balanced learning of desired visual semantics. The experimental results show that MagicTailor achieves superior performance in this task and enables more personalized and creative image generation.

1 Introduction

Text-to-image (T2I) diffusion models [Rombach *et al.*, 2022; Ramesh *et al.*, 2022; Chen *et al.*, 2023] have shown impressive capabilities in generating high-quality images from textual descriptions. While these models can generate images that align well with provided prompts, they struggle when certain visual concepts are hard to express in natural language. To address this, methods like [Gal *et al.*, 2022; Ruiz *et al.*, 2023] enable T2I models to learn specific concepts from a few reference images, allowing for more accurate integration of those concepts into the generated images. This process, as shown in Fig. 1(a), is referred as personalization.

However, existing personalization methods are limited to replicating predefined concepts and lack flexible and fine-grained control of these concepts. Such a limitation hinders their practical use in real-world applications, restricting their potential for creative expression. Inspired by the observation that concepts often comprise multiple components, a key problem in personalization lies in *how to effectively control and manipulate these individual components*.

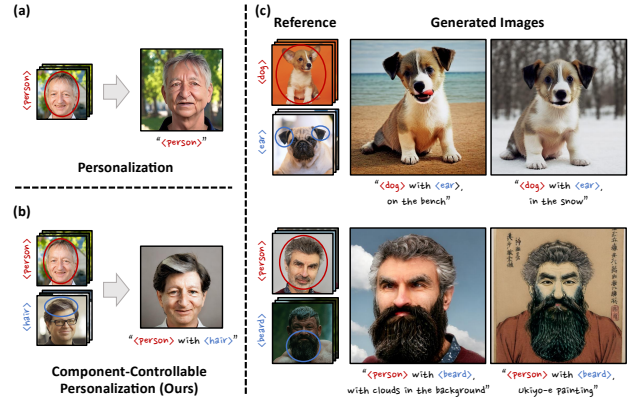


Figure 1: (a) **Personalization**: T2I models learn from reference images and then generate predefined visual concepts. (b) **Component-controllable personalization**: T2I models learn from additional visual references and then enable the integration of specific components into given concepts, further unleashing creativity. (c) **Generated images by MagicTailor**: MagicTailor can effectively achieve component-controllable personalization. Note that red and blue circles indicate the target concept and component, respectively.

In this paper, we introduce **component-controllable personalization**, a new task that enables the reconfiguration of specific components within personalized concepts using additional visual references (Fig. 1(b)). In this approach, a T2I model is fine-tuned with reference images and corresponding category labels, allowing it to learn and generate the desired concept along with the given component. This capability empowers users to refine and customize concepts with precise control, fostering creativity and innovation across various domains, from artworks to inventions.

One challenge of this task is *semantic pollution* (Fig. 2(a)), where unwanted visual elements inadvertently appear in generated images, “polluting” the personalized concept. This happens because the T2I model often mixes visual semantics from different regions during training. Masking out unwanted elements in reference images doesn’t solve the problem, as it disrupts the visual context and causes unintended compositions. Another challenge is *semantic imbalance* (Fig. 2(b)), where the model overemphasizes certain aspects, leading to unfaithful personalization. This occurs due to the semantic disparity between the concept and component, necessitating a more balanced learning approach to manage concept-level (e.g., person) and component-level (e.g., hair) semantics.

* Equal contribution. † Corresponding author.

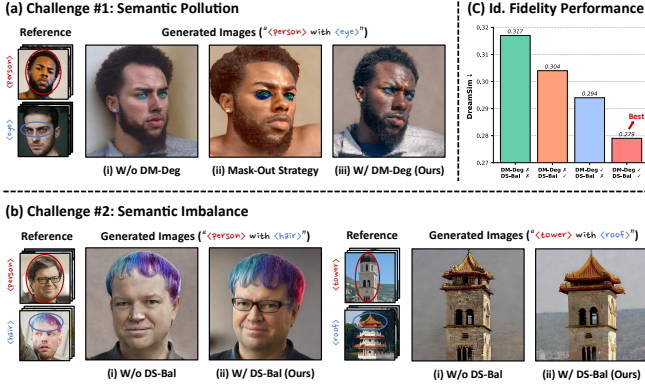


Figure 2: **Major challenges in component-controllable personalization.** (a) **Semantic pollution:** (i) Undesired elements may interfere with the personalized concept. (ii) A simple mask-out strategy causes unintended results, while (iii) DM-Deg effectively suppresses unwanted semantics. (b) **Semantic imbalance:** (i) Simultaneously learning the concept and component can distort either one. (ii) DS-Bal ensures balanced learning, improving personalization. (c) **Identity fidelity performance:** Calculating DreamSim [Fu et al., 2023] scores on our collected dataset, we show that DM-Deg and DS-Bal can address these challenges for faithful generation.

To address these challenges, we propose **MagicTailor**, a novel framework that enables component-controllable personalization for T2I models (Fig. 1(c)). We first use a text-guided image segmenter to generate segmentation masks for both the concept and component and then design *Dynamic Masked Degradation* (DM-Deg) to transform reference images into randomly degraded versions, perturbing undesired visual semantics. This method helps suppress the model’s sensitivity to irrelevant details while preserving the overall visual context, effectively mitigating *semantic pollution*. Next, we initiate a warm-up phase for the T2I model, training it on the degraded images using a masked diffusion loss to focus on the desired semantics and a cross-attention loss to strengthen the correlation between these semantics and pseudo-words. To address *semantic imbalance*, we develop *Dual-Stream Balancing* (DS-Bal), a dual-stream learning paradigm that balances the learning of visual semantics. In this phase, the online denoising U-Net performs sample-wise min-max optimization, while the momentum denoising U-Net applies selective preservation regularization. This ensures more faithful personalization of the target concept and component, resulting in outputs that better align with the intended objective.

In the experiments, we validate the superiority of MagicTailor through various qualitative and quantitative comparisons, demonstrating its state-of-the-art (SOTA) performance in component-controllable personalization. Moreover, detailed ablation studies and analysis further confirm the effectiveness of MagicTailor. In addition, we also show its potential for enabling a wide range of creative applications.

2 Related Works

Text-to-Image Generation. T2I generation has made remarkable advancements in recent years, enabling the synthesis of vivid and diverse imagery based on textual descriptions. Early methods employed Generative Adversarial Networks

(GANs) [Reed et al., 2016; Xu et al., 2018], and transformers [Ding et al., 2021; Yu et al., 2022; Bai et al., 2024] also showed the potential in conditional generation. The advent of diffusion models has ushered in a new era in T2I generation [Li et al., 2024; Saharia et al., 2022; Ramesh et al., 2022; Chen et al., 2023; Xue et al., 2024]. Leveraging these models, a range of related applications has rapidly emerged, including image editing [Li et al., 2024; Mou et al., 2024; Huang et al., 2024b; Feng et al., 2024; Huang et al., 2024a], image completion and translation [Xie et al., 2023b,a; Lin et al., 2024], and controllable image generation [Zhang et al., 2023; Wang et al., 2024; Zheng et al., 2023]. Despite advancements in T2I diffusion models, generating images that accurately reflect specific, user-defined concepts remains a challenge. This study explores component-controllable personalization, which allows precise adjustment of specific concepts’ components using visual references.

Personalization. Personalization seeks to adapt T2I models to generate given concepts using reference images. Initial approaches [Gal et al., 2022; Ruiz et al., 2023] addressed this task by either optimizing text embeddings or fine-tuning the entire T2I model. Additionally, low-rank adaptation (LoRA) [Hu et al., 2021] has been widely adopted in this field [Ryu, 2022], providing an efficient solution. The scope of personalization has expanded to encompass multiple concepts [Kumari et al., 2023; Avrahami et al., 2023; Gu et al., 2024; Ng et al., 2025]. Besides, several studies [Li et al., 2023; Wei et al., 2023; Zhang et al., 2024b; Song et al., 2024] have explored tuning-free approaches for personalization, but these necessitate additional training on large-scale image datasets [Zhang et al., 2024a]. In contrast, *MagicTailor is a tuning-base method that requires only a few images and leverages test-time optimization to enable stable performance.* Notably, several works [Huang et al., 2024c; Safaee et al., 2024; Ng et al., 2025] have also explored how to learn and customize fine-grained elements. However, these methods can only combine elements or process one element at the same level. By comparison, *MagicTailor is a versatile framework able to handle both component-level and concept-level elements.*

3 Methodology

Let $\mathcal{I} = \{(\{I_{nk}\}_{k=1}^K, c_n)\}_{n=1}^N$ denote a concept-component pair with N samples of concepts and components, where each sample contains K reference images $\{I_{nk}\}_{k=1}^K$ with a category label c_n . In this work, we focus on a practical setting involving one concept and one component. Specifically, we set $N = 2$ and define the first sample as a concept (e.g., dog) while the second one as a component (e.g., ear). In addition, these samples are associated with the pseudo-words $\mathcal{P} = \{p_n\}_{n=1}^N$ serving as their text identifiers. The goal of *component-controllable personalization* is to fine-tune a text-to-image (T2I) model to accurately learn both the concept and the component from \mathcal{I} . Using text prompts with \mathcal{P} , the fine-tuned model should generate images that integrate the personalized concept with the specified component.

This section begins by providing an overview of the MagicTailor pipeline in Sec. 3.1 and then delves into its two core techniques in Sec. 3.2 and Sec. 3.3.

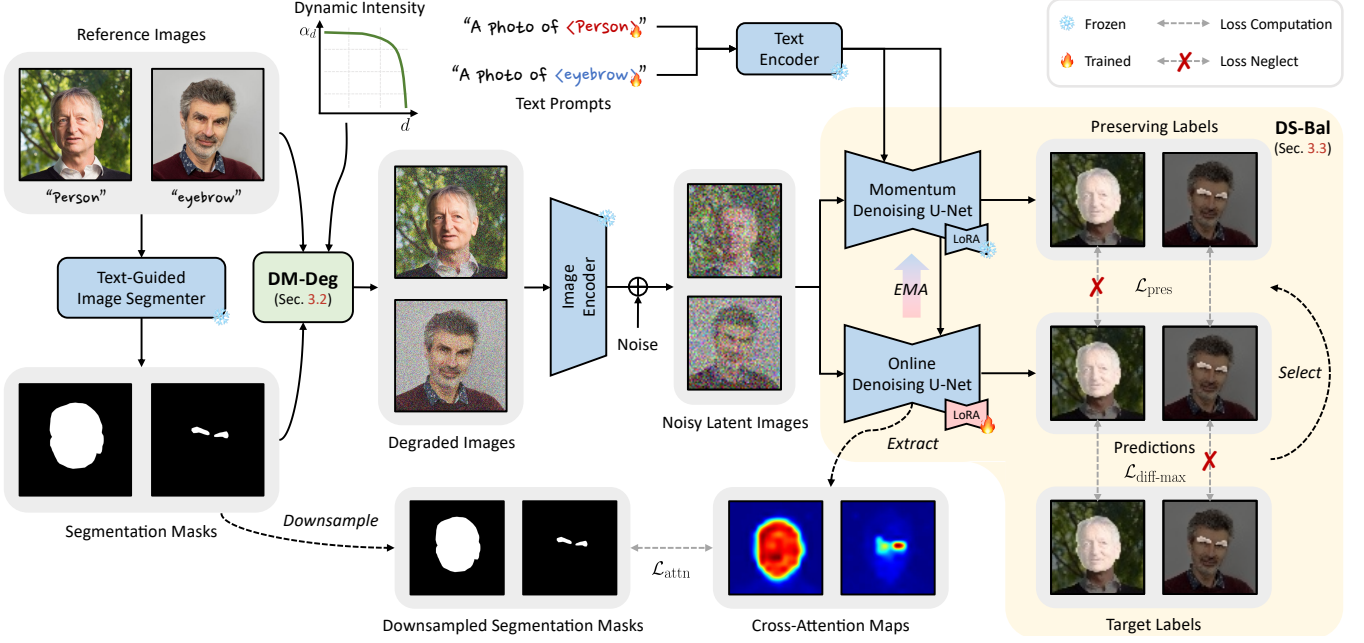


Figure 3: **Pipeline overview of MagicTailor.** This method fine-tunes a T2I diffusion model using reference images to learn both the target concept and component, enabling the generation of images that seamlessly integrate the component into the concept. Two key techniques, *Dynamic Masked Degradation (DM-Deg)*, see Sec. 3.2) and *Dual-Stream Balancing (DS-Bal)*, see Sec. 3.3), address *semantic pollution* and *semantic imbalance*, respectively. For clarity, only one image per concept/component is shown, and the warm-up stage is omitted.

3.1 Overall Pipeline

The overall pipeline of MagicTailor is illustrated in Fig. 3. The process begins with identifying the desired concept or component within each reference image I_{nk} , employing an off-the-shelf text-guided image segmenter to generate a segmentation mask M_{nk} based on I_{nk} and its associated category label c_n . Conditioned on M_{nk} , we design *Dynamic Masked Degradation (DM-Deg)* to perturb undesired visual semantics within I_{nk} , addressing *semantic pollution*. At each training step, DM-Deg transforms I_{nk} into a randomly degraded image \hat{I}_{nk} , with the degradation intensity being dynamically regulated. Subsequently, these degraded images, along with structured text prompts, are used to fine-tune a T2I diffusion model to facilitate concept and component learning. The model is formally expressed as $\{\epsilon_\theta, \tau_\theta, \mathcal{E}, \mathcal{D}\}$, where ϵ_θ represents the denoising U-Net, τ_θ is the text encoder, and \mathcal{E} and \mathcal{D} denote the image encoder and decoder, respectively. To promote the learning of the desired visual semantics, we employ the masked diffusion loss, which is defined as:

$$\mathcal{L}_{\text{diff}} = \mathbb{E}_{n,k,\epsilon,t} \left[\left\| \epsilon_n \odot M'_{nk} - \epsilon_\theta(z_{nk}^{(t)}, t, e_n) \odot M'_{nk} \right\|_2^2 \right], \quad (1)$$

where $\epsilon_n \sim \mathcal{N}(0, 1)$ is the unscaled noise, $z_{nk}^{(t)}$ is the noisy latent image of \hat{I}_{nk} with a random time step t , e_n is the text embedding of the corresponding text prompt, and M'_{nk} is downsampled from M_{nk} to match the shape of ϵ and z_{nk} . Additionally, we incorporate the cross-attention loss to strengthen the correlation between desired visual semantics and their corresponding pseudo-words, formulated as:

$$\mathcal{L}_{\text{attn}} = \mathbb{E}_{n,k,t} \left[\left\| A_\theta(p_n, z_{nk}^{(t)}) - M''_{nk} \right\|_2^2 \right], \quad (2)$$

when $A_\theta(p_n, z_{nk}^{(t)})$ is the cross-attention maps between the pseudo-word p_n and the noisy latent image $z_{nk}^{(t)}$ and M''_{nk} is downsampled from M_{nk} to match the shape of $A_\theta(p_n, z_{nk}^{(t)})$.

Using $\mathcal{L}_{\text{diff}}$ and $\mathcal{L}_{\text{attn}}$, we first warm up the T2I model by jointly learning all samples, aiming to preliminarily inject the knowledge of visual semantics. The loss of the warm-up stage is defined as:

$$\mathcal{L}_{\text{warm-up}} = \mathcal{L}_{\text{diff}} + \lambda_{\text{attn}} \mathcal{L}_{\text{attn}}, \quad (3)$$

where $\lambda_{\text{attn}} = 0.01$ is the loss weight for $\mathcal{L}_{\text{attn}}$. For efficient fine-tuning, we only train the denoising U-Net ϵ_θ in a low-rank adaptation (LoRA) [Hu et al., 2021] manner and the text embedding of the pseudo-words \mathcal{P} , keeping the others frozen. Thereafter, we employ *Dual-Stream Balancing (DS-Bal)* to address *semantic imbalance*. In this paradigm, the online denoising U-Net ϵ_θ conducts sample-wise min-max optimization for the hardest-to-learn sample, and meanwhile the momentum denoising U-Net $\tilde{\epsilon}_\theta$ applies selective preserving regularization for the other samples.

3.2 Dynamic Masked Degradation

Semantic pollution is a significant challenge for component-controllable personalization. As shown in Fig. 2(a.i), the target concept (i.e., person) can be distorted by the owner of the target component (i.e., eye), resulting in a hybrid person. Masking regions outside the target concept and component can damage the overall context, leading to overfitting and odd compositions (Fig. 2(a.ii)). To address this, undesired visual semantics in reference images must be handled appropriately. We propose *Dynamic Masked Degradation (DM-Deg)*, which dynamically perturbs undesired semantics to suppress their

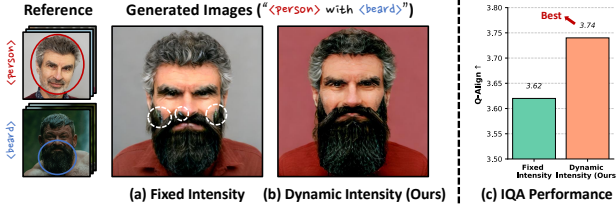


Figure 4: **Motivation of dynamic intensity.** (a) Fixed intensity ($\alpha_d = 0.5$ here) could cause noisy generated images. (b) Our dynamic intensity can mitigate noise memorization. (c) We report IQA results of Q-Align [Wu *et al.*, 2023] on our dataset, showing that our dynamic intensity helps to enhance the quality of generated images.

influence on the T2I model while preserving the overall visual context (Fig. 2(a.iii)&(c)).

Degradation Imposition. In each training step, DM-Deg imposes degradation in the out-of-mask region for each reference image. We use Gaussian noise for degradation due to its simplicity. For a reference image I_{nk} , we randomly sample a Gaussian noise matrix $G_{nk} \sim \mathcal{N}(0, 1)$ with the same shape as I_{nk} , where the pixel values of I_{nk} range from -1 to 1 . The degradation is then applied as follows:

$$\hat{I}_{nk} = \alpha_d G_{nk} \odot (1 - M_{nk}) + I_{nk}, \quad (4)$$

where \odot denotes element-wise multiplication, and $\alpha_d \in [0, 1]$ is a dynamic weight controlling the degradation intensity. While previous works [Xiao *et al.*, 2023; Li *et al.*, 2023] have used noise to fully cover the background or enhance data diversity, DM-Deg aims to produce a degraded image \hat{I}_{nk} that retains the original visual context. By introducing \hat{I}_{nk} , we can suppress the T2I model from perceiving undesired visual semantics in out-of-mask regions, as these semantics are perturbed by random noise at each training step.

Dynamic Intensity. Unfortunately, the T2I model may gradually memorize the introduced noise while learning meaningful visual semantics, leading to noise appearing in generated images (Fig. 4(a)). This behavior is consistent with previous observations on deep networks [Arpit *et al.*, 2017]. To address this, we propose a descending scheme that dynamically regulates the intensity of the imposed noise during training. This scheme follows an exponential curve, maintaining a relatively high intensity in the early stages and decreasing it sharply in later stages. Let d denote the current training step and D denote the total training step. The curve of dynamic intensity is defined as:

$$\alpha_d = \alpha_{\text{init}} \left(1 - \left(\frac{d}{D}\right)^\gamma\right), \quad (5)$$

where α_{init} is the initial value of α_d and γ controls the descent rate. We empirically set $\alpha_{\text{init}} = 0.5$ and $\gamma = 32$, tuned within the powers of 2. This dynamic intensity scheme effectively prevents semantic pollution and significantly mitigates the memorization of introduced noise, leading to improved generation performance (Fig. 4(b)&(c)).

3.3 Dual-Stream Balancing

Another key challenge is *semantic imbalance*, which arises from the disparity in visual semantics between the target concept and its component. Specifically, concepts generally possess richer visual semantics than components (e.g., person vs.

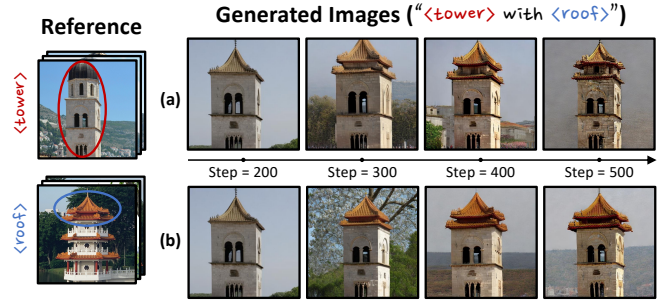


Figure 5: **Learning process visualization.** (a) The vanilla learning paradigm tends to overemphasize the easier one. (b) DS-Bal effectively balances the learning of the concept and component.

hair), but in some cases, components may have more complex semantics (e.g., simple tower vs. intricate roof). This imbalance complicates joint learning, leading to overemphasis on either the concept or the component, and resulting in incoherent generation (Fig. 5(a)). To address this, we design *Dual-Stream Balancing (DS-Bal)*, a dual-stream learning paradigm integrated with online and momentum denoising U-Nets (Fig. 3) for balanced semantic learning, aiming to improve personalization fidelity (Fig. 5(b) & Fig. 2(c)).

Sample-Wise Min-Max Optimization. From a loss perspective, the visual semantics of the concept and component are learned by optimizing the masked diffusion loss $\mathcal{L}_{\text{diff}}$ across all the samples. However, this indiscriminate optimization fails to allocate sufficient learning effort to a more challenging sample, leading to an imbalanced learning process. To address this, DS-Bal uses the online denoising U-Net to focus on learning the hardest-to-learn sample at each training step. Inheriting the weights of the original denoising U-Net, which is warmed up through joint learning, the online denoising U-Net ϵ_θ optimizes only the sample with the highest masked diffusion loss as:

$$\mathcal{L}_{\text{diff-max}} = \max_n \mathbb{E}_{k, \epsilon, t} \left[\left\| \epsilon_n \odot M'_{nk} - \epsilon_\theta(z_{nk}^{(t)}, t, e_n) \odot M'_{nk} \right\|_2^2 \right], \quad (6)$$

where minimizing $\mathcal{L}_{\text{diff-max}}$ can be considered as a form of min-max optimization [Razaviyayn *et al.*, 2020]. The learning objective of ϵ_θ may switch across different training steps and is not consistently dominated by the concept or component. Such an optimization scheme can effectively modulate the learning dynamics of multiple samples and avoid the overemphasis on any particular one.

Selective Preserving Regularization. At a training step, the sample neglected in $\mathcal{L}_{\text{diff-max}}$ may suffer from knowledge forgetting. This is because the optimization of $\mathcal{L}_{\text{diff-max}}$, which aims to enhance the knowledge of a specific sample, could inadvertently overshadow the knowledge of the others. In light of this, DS-Bal meanwhile exploits the momentum denoising U-Net $\tilde{\epsilon}_\theta$ to preserve the learned visual semantics of the other sample in each training step. Specifically, we first select the sample that is excluded in $\mathcal{L}_{\text{diff-max}}$, which is expressed as $S = \{n | n = 1, \dots, N\} - \{n_{\text{max}}\}$, where n_{max} is the index of the target sample in $\mathcal{L}_{\text{diff-max}}$ and S is the selected

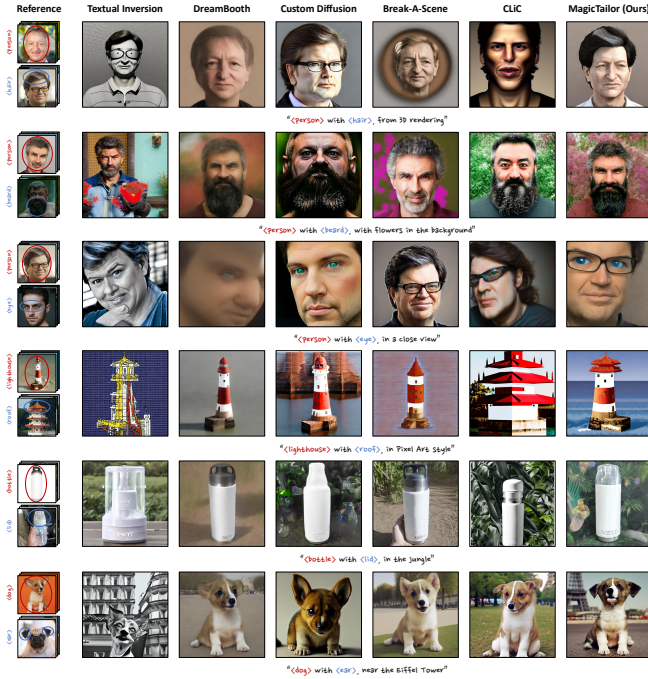


Figure 6: **Qualitative comparisons.** We present images generated by MagicTailor and other methods across various domains. MagicTailor achieves better text alignment, identity fidelity, and generation quality. *Due to space limitations, please zoom in for a better view.* More results are provided in Appendix D.

index set. Then, we use $\tilde{\epsilon}_\theta$ to apply regularization for S , with the masked preserving loss as:

$$\mathcal{L}_{\text{pres}} = \mathbb{E}_{n \in S, k, t} \left[\left\| \tilde{\epsilon}_\theta(z_{nk}^{(t)}, t, e_n) \odot M'_{nk} - \epsilon_\theta(z_{nk}^{(t)}, t, e_n) \odot M'_{nk} \right\|_2^2 \right], \quad (7)$$

where $\tilde{\epsilon}_\theta$ is updated from ϵ_θ using EMA [Tarvainen and Valpola, 2017] with the smoothing coefficient $\beta = 0.99$, thereby sustaining the prior accumulated knowledge of ϵ_θ in each training step. By encouraging the consistency between the output of ϵ_θ and $\tilde{\epsilon}_\theta$ in $\mathcal{L}_{\text{pres}}$, we can facilitate the knowledge maintenance of the other samples while learning a specific sample in $\mathcal{L}_{\text{diff-max}}$. Overall, DS-Bal can be considered a mechanism to adaptively assign target labels ϵ_n or preserving labels $\tilde{\epsilon}_\theta(z_{nk}^{(t)}, t, e_n)$ to different samples, enabling dynamic loss supervision (Fig. 3). Using a loss weight $\lambda_{\text{pres}} = 0.2$, the total loss of the DS-Bal stage is formulated as:

$$\mathcal{L}_{\text{DS-Bal}} = \mathcal{L}_{\text{diff-max}} + \lambda_{\text{pres}} \mathcal{L}_{\text{pres}} + \lambda_{\text{attn}} \mathcal{L}_{\text{attn}}. \quad (8)$$

4 Experimental Results

4.1 Experimental Setup

Dataset, Implementation, and Evaluation. For a systematic investigation, we collect a dataset from diverse domains, including characters, animation, buildings, objects, and animals. We use Stable Diffusion (SD) 2.1 [Rombach *et al.*, 2022] as the pretrained T2I model. For the warm-up and DS-Bal stages, we set the training steps to 200 and 300, with learning rates of 1×10^{-4} and 1×10^{-5} , respectively. Each

Table 1: **Quantitative comparisons on automatic metrics.** MagicTailor can achieve SOTA performance on all four automatic metrics. The best results are marked in bold.

Methods	CLIP-T \uparrow	CLIP-I \uparrow	DINO \uparrow	DreamSim \downarrow
Textual Inversion [Gal <i>et al.</i> , 2022]	0.236	0.742	0.620	0.558
DreamBooth [Ruiz <i>et al.</i> , 2023]	0.266	0.841	0.798	0.323
Custom Diffusion [Kumari <i>et al.</i> , 2023]	0.251	0.797	0.750	0.407
Break-A-Scene [Avrahami <i>et al.</i> , 2023]	0.259	0.840	0.780	0.338
CLiC [Safaei <i>et al.</i> , 2024]	0.263	0.764	0.663	0.499
MagicTailor (Ours)	0.270	0.854	0.813	0.279

Table 2: **Quantitative comparisons on the user study.** MagicTailor also outperforms other methods in all aspects of human evaluation.

Methods	Text Align. \uparrow	Id. Fidelity \uparrow	Gen. Quality \uparrow
Textual Inversion [Gal <i>et al.</i> , 2022]	5.8%	2.5%	5.2%
DreamBooth [Ruiz <i>et al.</i> , 2023]	15.3%	14.7%	12.5%
Custom Diffusion [Kumari <i>et al.</i> , 2023]	7.1%	7.7%	9.8%
Break-A-Scene [Avrahami <i>et al.</i> , 2023]	10.8%	12.1%	22.8%
CLiC [Safaei <i>et al.</i> , 2024]	4.5%	5.1%	6.2%
MagicTailor (Ours)	56.5%	57.9%	43.4%

concept-component pair requires only about five minutes of training on an A100 GPU. For evaluation, we design 20 text prompts covering a wide range of scenarios and generate 14,720 images for each method. To ensure fairness, all random seeds are fixed during both training and inference. More details of the experimental setup are included in Appendix A.

Compared Methods. We compare our MagicTailor with several personalization methods, including Textual Inversion (TI) [Gal *et al.*, 2022], DreamBooth (DB) [Ruiz *et al.*, 2023], Custom Diffusion (CD) [Kumari *et al.*, 2023], Break-A-Scene (BAS) [Avrahami *et al.*, 2023], and CLiC [Safaei *et al.*, 2024]. These methods were selected for their representativeness of personalization frameworks or relevance to learning fine-grained elements. For a fair comparison, we adapt them to our task with minimal modifications, specifically by incorporating the masked diffusion loss (Eq. 1). Apart from method-specific configurations, all methods are implemented using the same setup to ensure consistency.

4.2 Qualitative Comparisons

The qualitative results are shown in in Fig. 6. As observed, TI, CD, and CLiC primarily suffer from semantic pollution, where undesired visual semantics significantly distort the personalized concept. Besides, DB and BAS also struggle in this challenging task, with an overemphasis on either the concept or the component due to semantic imbalance, sometimes even causing the target component to be completely absent. An interesting finding is that imbalanced learning can exacerbate semantic pollution, leading to the color and texture of the target concept or component being mistakenly transferred to unintended parts of the generated images. In contrast, MagicTailor effectively generates text-aligned images that accurately represent both the target concept and component. To further demonstrate the performance of MagicTailor, we provide additional comparisons in Appendix B.

Table 3: **Effectiveness of key techniques.** Our DM-Deg and DS-Bal effectively contribute to a superior performance trade-off.

DM-Deg	DS-Bal	CLIP-T \uparrow	CLIP-I \uparrow	DINO \uparrow	DreamSim \downarrow
		0.275	0.837	0.798	0.317
✓		0.276	0.848	0.809	0.294
	✓	0.270	0.845	0.802	0.304
✓	✓	0.270	0.854	0.813	0.279



Figure 7: **Compatibility with different backbones.** We equip MagicTailor with SD 1.5 [Rombach *et al.*, 2022], SD 2.1 [Rombach *et al.*, 2022], and SDXL [Podell *et al.*, 2023]. The results show that MagicTailor can be generalized to multiple backbones, and a better backbone could provide better generation quality.

4.3 Quantitative Comparisons

Automatic Metrics. We utilize four automatic metrics in the aspects of text alignment (CLIP-T [Gal *et al.*, 2022]) and identity fidelity (CLIP-I [Radford *et al.*, 2021], DINO [Oquab *et al.*, 2023], DreamSim [Fu *et al.*, 2023]). *To precisely measure identity fidelity*, we segment out the concept and component in each reference and evaluation image, and then eliminate the target component from the segmented concept. As we can see in Tab. 1, component-controllable personalization remains a tough task even for SOTA methods of personalization. By comparison, MagicTailor achieves the best results in both identity fidelity and text alignment. It should be credited to the effective framework tailored to this special task.

User Study. We further evaluate the methods with a user study. Specifically, a detailed questionnaire is designed to display 20 groups of evaluation images with the corresponding text prompt and reference images. Users are asked to select the best result in each group for three aspects, including text alignment, identity fidelity, and generation quality. Finally, we collect a total of 3,180 valid answers and report the selected rates in Tab. 2. It can be observed that MagicTailor can also achieve superior performance in human preferences, further verifying its effectiveness.

4.4 Ablation Studies and Analysis

We conduct comprehensive ablation studies and analysis for MagicTailor to verify its capability. More ablation studies and analysis are included in Appendix C.

Effectiveness of Key Techniques. In Tab. 3, we investigate two key techniques by starting from a baseline framework described in Sec. 3.1. Even without DM-Deg and DS-Bal, such a baseline framework can still have competitive performance,

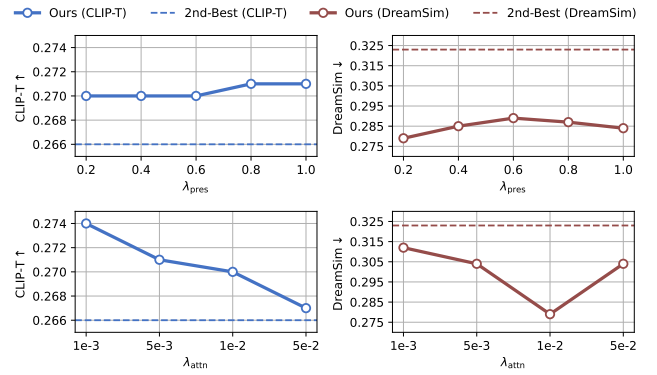


Figure 8: **Robustness on loss weights.** We report CLIP-T [Gal *et al.*, 2022] for text alignment, and DreamSim [Fu *et al.*, 2023] for identity fidelity as it is most similar to human judgments. Second-best results in Table 1 are also presented to highlight our robustness.

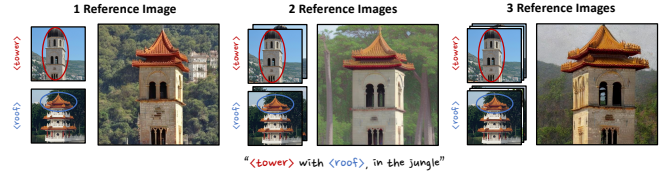


Figure 9: **Performance on different numbers of reference images.** We present qualitative results to show that MagicTailor can still achieve satisfactory performance when provided only 1 or 2 reference image(s) per concept and component.c

showing its reliability. On top of that, we introduce DM-Deg and DS-Bal, where the superior performance trade-off indicates their significance. Qualitative results can refer to Fig. 2.

Compatibility with Different Backbones. MagicTailor can also collaborate with other T2I diffusion models as it is a model-independent approach. In Fig. 7, we employ MagicTailor in other backbones like SD 1.5 [Rombach *et al.*, 2022] and SDXL [Podell *et al.*, 2023], showcasing MagicTailor can also achieve remarkable results. Notably, we directly use the original hyperparameter values without further selections, showing the generalizability of MagicTailor.

Robustness on Loss Weights. In Fig. 8, we analyze the sensitivity of loss weights in Eq. 8 (*i.e.*, λ_{pres} and λ_{attn}), since loss weights are often critical for model training. As we can see, when λ_{pres} and λ_{attn} vary within a reasonable range, our MagicTailor can consistently attain SOTA performance, revealing its robustness on these hyperparameters.

Performance on Different Numbers of Reference Images. In Fig. 9, we reduce the number of reference images to analyze the performance variation. With fewer reference images, MagicTailor can still show satisfactory results. While more reference images could lead to better generalization ability, one reference image per concept/component is enough to obtain a decent result with our MagicTailor.

Generalizability to Complex Prompts. In comparisons, we have used well-categorized text prompts for systemic evaluation. Here we further evaluate MagicTailor’s performance on other complex text prompts involving more complicated contexts. As shown in Fig. 11, MagicTailor effectively generates text-aligned images when performing fidelity personalization, showing its ability to handle diverse user needs.

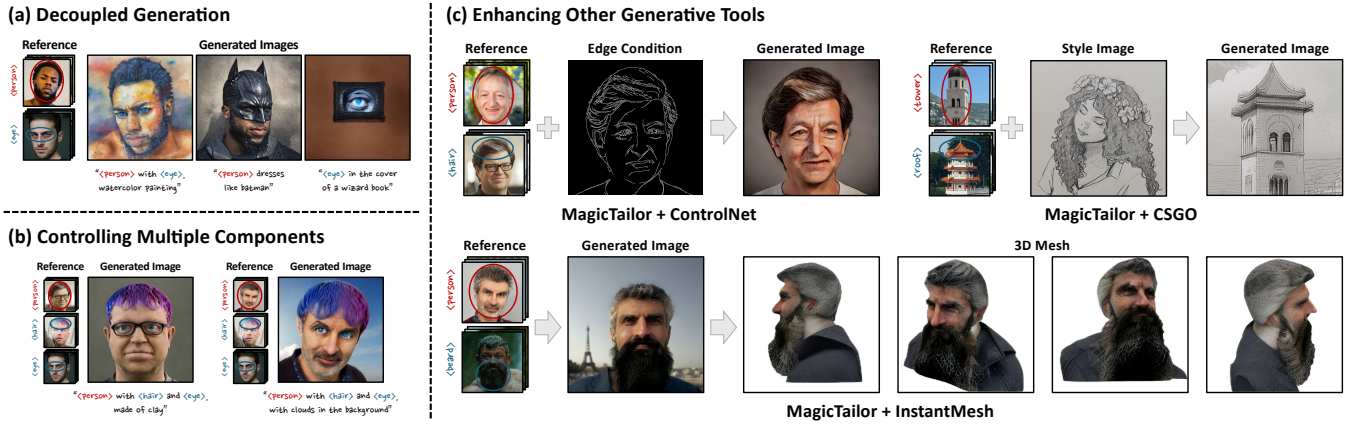


Figure 10: **Further applications of MagicTailor.** (a) **Decoupled generation:** MagicTailor can also separately generate the target concept and component, enriching prospective combinations. (b) **Controlling multiple components:** MagicTailor shows the potential to handle more than one component, highlighting its effectiveness. (c) **Enhancing other generative tools:** MagicTailor can seamlessly integrate with various generative tools, adding the capability to control components within their generation pipelines.

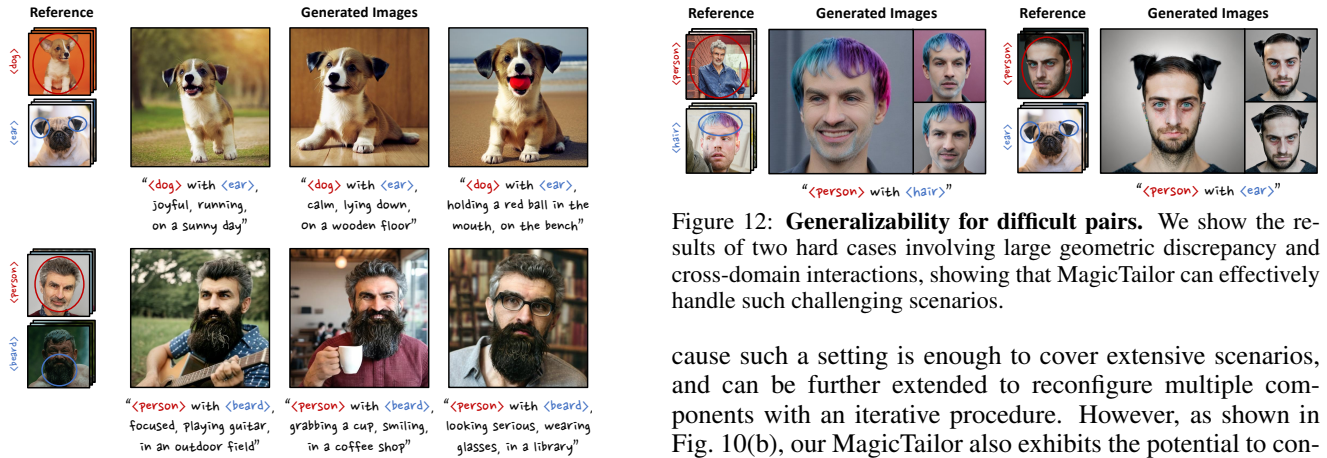


Figure 11: **Generalizability for complex prompts.** We present qualitative results generated with complex text prompts. In addition to those well-categorized text prompts, our MagicTailor can also follow more complex ones to generate text-aligned images.

Generalizability to Difficult Pairs. We further evaluate MagicTailor’s performance on challenging pairs, focusing on two cases: 1) large geometric discrepancy, such as “<person>” in an upper body portrait and “<hair>” in a profile photo, and 2) cross-domain interactions, such as “<person>” and “<ear>” of dogs. As shown in Fig. 12, even facing these hard cases, MagicTailor can still effectively personalize target concepts and components with high fidelity.

4.5 Further Applications

Decoupled Generation. After learning from a concept-component pair, MagicTailor can also enable decoupled generation. As shown in Fig. 10(a), MagicTailor can generate the target concept and component separately in various and even cross-domain contexts. This should be credited to its remarkable ability to capture different-level visual semantics. Such an ability extends the flexibility of the possible combination between the concept and component.

Controlling Multiple Components. In this paper, we focus on personalizing one concept and one component, be-

Figure 12: **Generalizability for difficult pairs.** We show the results of two hard cases involving large geometric discrepancy and cross-domain interactions, showing that MagicTailor can effectively handle such challenging scenarios.

cause such a setting is enough to cover extensive scenarios, and can be further extended to reconfigure multiple components with an iterative procedure. However, as shown in Fig. 10(b), our MagicTailor also exhibits the potential to control two components simultaneously. Handling more components remains a prospective direction of exploring better control over diverse elements for a single concept.

Enhancing Other Generative Tools. We demonstrate how MagicTailor enhances other generative tools like ControlNet [Zhang *et al.*, 2023], CSGO [Xing *et al.*, 2024], and InstantMesh [Xu *et al.*, 2024] in Fig. 10(c). MagicTailor can integrate seamlessly, furnishing them with an additional ability to control the concept’s component in their pipelines. For instance, working with MagicTailor, InstantMesh can conveniently achieve fine-grained 3D mesh design, exhibiting the practicability of MagicTailor in more creative applications.

5 Conclusion

We introduce *component-controllable personalization*, enabling precise customization of individual components within concepts. The proposed *MagicTailor* uses *Dynamic Masked Degradation (DM-Deg)* to suppress unwanted semantics and *Dual-Stream Balancing (DS-Bal)* to ensure balanced learning. Experiments show that MagicTailor sets a new standard in this task, with promising creative applications. In the future, we would like to extend our approach to broader image and video generation, enabling finer control over multi-level visual semantics for creative generation capabilities.

Acknowledgments

We would like to thank Pengzhi Li, Tian Ye, Jinyu Lin, and Jialin Gao for their valuable discussion and suggestions. This study was supported by the InnoHK initiative of the Innovation and Technology Commission of the Hong Kong Special Administrative Region Government via the Hong Kong Centre for Logistics Robotics.

References

- Devansh Arpit, Stanislaw Jastrzebski, Nicolas Ballas, David Krueger, Emmanuel Bengio, Maxinder S Kanwal, Tegan Maharaj, Asja Fischer, Aaron Courville, Yoshua Bengio, et al. A closer look at memorization in deep networks. In *Int. Conf. Mach. Learn.*, pages 233–242, 2017.
- Omri Avrahami, Kfir Aberman, Ohad Fried, Daniel Cohen-Or, and Dani Lischinski. Break-a-scene: Extracting multiple concepts from a single image. In *SIGGRAPH Asia*, pages 1–12, 2023.
- Jinbin Bai, Tian Ye, Wei Chow, Enxin Song, Qing-Guo Chen, Xiangtai Li, Zhen Dong, Lei Zhu, and Shuicheng Yan. Meissonic: Revitalizing masked generative transformers for efficient high-resolution text-to-image synthesis. *arXiv preprint arXiv:2410.08261*, 2024.
- Junsong Chen, Jincheng Yu, Chongjian Ge, Lewei Yao, Enze Xie, Yue Wu, Zhongdao Wang, James Kwok, Ping Luo, Huchuan Lu, et al. Pixart- α : Fast training of diffusion transformer for photorealistic text-to-image synthesis. *arXiv preprint arXiv:2310.00426*, 2023.
- Ming Ding, Zhuoyi Yang, Wenyi Hong, Wendi Zheng, Chang Zhou, Da Yin, Junyang Lin, Xu Zou, Zhou Shao, Hongxia Yang, et al. Cogview: Mastering text-to-image generation via transformers. In *Adv. Neural Inf. Process. Syst.*, pages 19822–19835, 2021.
- Hugging Face. Diffusers: State-of-the-art diffusion models for image and audio generation in pytorch and flax., 2022.
- Aosong Feng, Weikang Qiu, Jinbin Bai, Kaicheng Zhou, Zhen Dong, Xiao Zhang, Rex Ying, and Leandros Tassiulas. An item is worth a prompt: Versatile image editing with disentangled control. *arXiv preprint arXiv:2403.04880*, 2024.
- Stephanie Fu, Netanel Tamir, Shobhita Sundaram, Lucy Chai, Richard Zhang, Tali Dekel, and Phillip Isola. Dreamsim: Learning new dimensions of human visual similarity using synthetic data. *arXiv preprint arXiv:2306.09344*, 2023.
- Rinon Gal, Yuval Alaluf, Yuval Atzmon, Or Patashnik, Amit Haim Bermano, Gal Chechik, and Daniel Cohen-or. An image is worth one word: Personalizing text-to-image generation using textual inversion. In *Int. Conf. Learn. Represent.*, 2022.
- Yuchao Gu, Xintao Wang, Jay Zhangjie Wu, Yujun Shi, Yunpeng Chen, Zihan Fan, Wuyou Xiao, Rui Zhao, Shuning Chang, Weijia Wu, et al. Mix-of-show: Decentralized low-rank adaptation for multi-concept customization of diffusion models. In *Adv. Neural Inf. Process. Syst.*, 2024.
- Jonathan Ho, Ajay Jain, and Pieter Abbeel. Denoising diffusion probabilistic models. In *Adv. Neural Inf. Process. Syst.*, pages 6840–6851, 2020.
- Edward J. Hu, Yelong Shen, Phillip Wallis, Zeyuan Allen-Zhu, Yanzhi Li, Shean Wang, Lu Wang, and Weizhu Chen. Lora: Low-rank adaptation of large language models. *arXiv preprint arXiv:2106.09685*, 2021.
- Jiancheng Huang, Yi Huang, Jianzhuang Liu, Donghao Zhou, Yifan Liu, and Shifeng Chen. Dual-schedule inversion: Training-and tuning-free inversion for real image editing. *arXiv preprint arXiv:2412.11152*, 2024.
- Yi Huang, Jiancheng Huang, Yifan Liu, Mingfu Yan, Jiayi Lv, Jianzhuang Liu, Wei Xiong, He Zhang, Shifeng Chen, and Liangliang Cao. Diffusion model-based image editing: A survey. *arXiv preprint arXiv:2402.17525*, 2024.
- Zehuan Huang, Hongxing Fan, Lipeng Wang, and Lu Sheng. From parts to whole: A unified reference framework for controllable human image generation. *arXiv preprint arXiv:2404.15267*, 2024.
- Aaron Hurst, Adam Lerer, Adam P Goucher, Adam Perelman, Aditya Ramesh, Aidan Clark, AJ Ostrow, Akila Welihinda, Alan Hayes, Alec Radford, et al. Gpt-4o system card. *arXiv preprint arXiv:2410.21276*, 2024.
- Jimyong Kim, Jungwon Park, and Wonjong Rhee. Selectively informative description can reduce undesired embedding entanglements in text-to-image personalization. In *Proceedings of the IEEE/CVF Conference on Computer Vision and Pattern Recognition*, pages 8312–8322, 2024.
- Nupur Kumari, Bingliang Zhang, Richard Zhang, Eli Shechtman, and Jun-Yan Zhu. Multi-concept customization of text-to-image diffusion. In *IEEE Conf. Comput. Vis. Pattern Recognit.*, pages 1931–1941, 2023.
- Zhen Li, Mingdeng Cao, Xintao Wang, Zhongang Qi, Ming-Ming Cheng, and Ying Shan. Photomaker: Customizing realistic human photos via stacked id embedding. *arXiv preprint arXiv:2312.04461*, 2023.
- Pengzhi Li, Qiang Nie, Ying Chen, Xi Jiang, Kai Wu, Yuhuan Lin, Yong Liu, Jinlong Peng, Chengjie Wang, and Feng Zheng. Tuning-free image customization with image and text guidance. *arXiv preprint arXiv:2403.12658*, 2024.
- Jingyu Lin, Guiqin Zhao, Jing Xu, Guoli Wang, Zejin Wang, Antitza Dantcheva, Lan Du, and Cunjian Chen. Diffvt: Identity-preserved thermal-to-visible face translation via feature alignment and dual-stage conditions. In *ACM Int. Conf. Multimedia*, 2024.
- Ilya Loshchilov and Frank Hutter. Decoupled weight decay regularization. *arXiv preprint arXiv:1711.05101*, 2017.
- Chong Mou, Xintao Wang, Jiechong Song, Ying Shan, and Jian Zhang. Diffeditor: Boosting accuracy and flexibility on diffusion-based image editing. *arXiv preprint arXiv:2402.02583*, 2024.
- Kam Woh Ng, Xiatian Zhu, Yi-Zhe Song, and Tao Xiang. Partcraft: Crafting creative objects by parts. In *European Conference on Computer Vision*, pages 420–437. Springer, 2025.

- Maxime Oquab, Timothée Darcet, Théo Moutakanni, Huy Vo, Marc Szafraniec, Vasil Khalidov, Pierre Fernandez, Daniel Haziza, Francisco Massa, Alaaeldin El-Nouby, et al. Dinov2: Learning robust visual features without supervision. *arXiv preprint arXiv:2304.07193*, 2023.
- Dustin Podell, Zion English, Kyle Lacey, Andreas Blattmann, Tim Dockhorn, Jonas Muller, Joe Penna, and Robin Rombach. Sdxl: Improving latent diffusion models for high-resolution image synthesis. *arXiv preprint arXiv:2307.01952*, 2023.
- Alec Radford, Jong Wook Kim, Chris Hallacy, Aditya Ramesh, Gabriel Goh, Sandhini Agarwal, Girish Sastry, Amanda Askell, Pamela Mishkin, Jack Clark, et al. Learning transferable visual models from natural language supervision. In *Int. Conf. Mach. Learn.*, pages 8748–8763, 2021.
- Aditya Ramesh, Prafulla Dhariwal, Alex Nichol, Casey Chu, and Mark Chen. Hierarchical text-conditional image generation with clip latents. *arXiv preprint arXiv:2204.06125*, 2022.
- Meisam Razaviyayn, Tianjian Huang, Songtao Lu, Maher Nouiehed, Maziar Sanjabi, and Mingyi Hong. Nonconvex min-max optimization: Applications, challenges, and recent theoretical advances. *IEEE Signal Process. Mag.*, 37(5):55–66, 2020.
- Scott Reed, Zeynep Akata, Xinchun Yan, Lajanugen Logeswaran, Bernt Schiele, and Honglak Lee. Generative adversarial text to image synthesis. In *Int. Conf. Mach. Learn.*, pages 1060–1069, 2016.
- Tianhe Ren, Shilong Liu, Ailing Zeng, Jing Lin, Kunchang Li, He Cao, Jiayu Chen, Xinyu Huang, Yukang Chen, Feng Yan, et al. Grounded sam: Assembling open-world models for diverse visual tasks. *arXiv preprint arXiv:2401.14159*, 2024.
- Robin Rombach, Andreas Blattmann, Dominik Lorenz, Patrick Esser, and Björn Ommer. High-resolution image synthesis with latent diffusion models. In *IEEE Conf. Comput. Vis. Pattern Recognit.*, pages 10684–10695, 2022.
- Nataniel Ruiz, Yuanzhen Li, Varun Jampani, Yael Pritch, Michael Rubinstein, and Kfir Aberman. Dreambooth: Fine tuning text-to-image diffusion models for subject-driven generation. In *IEEE Conf. Comput. Vis. Pattern Recognit.*, pages 22500–22510, 2023.
- Simo Ryu. Low-rank adaptation for fast text-to-image diffusion fine-tuning, 2022.
- Mehdi Safaei, Aryan Mikaeili, Or Patashnik, Daniel Cohen-Or, and Ali Mahdavi-Amiri. Clic: Concept learning in context. In *IEEE Conf. Comput. Vis. Pattern Recognit.*, pages 6924–6933, 2024.
- Chitwan Saharia, William Chan, Saurabh Saxena, Lala Li, Jay Whang, Emily L Denton, Kamyar Ghasemipour, Raphael Gontijo Lopes, Burcu Karagol Ayan, Tim Salimans, et al. Photorealistic text-to-image diffusion models with deep language understanding. *Adv. Neural Inf. Process. Syst.*, 35:36479–36494, 2022.
- Jiaming Song, Chenlin Meng, and Stefano Ermon. Denoising diffusion implicit models. *arXiv preprint arXiv:2010.02502*, 2020.
- Kunpeng Song, Yizhe Zhu, Bingchen Liu, Qing Yan, Ahmed Elgammal, and Xiao Yang. Moma: Multimodal llm adapter for fast personalized image generation. In *European Conference on Computer Vision*, pages 117–132. Springer, 2024.
- Antti Tarvainen and Harri Valpola. Mean teachers are better role models: Weight-averaged consistency targets improve semi-supervised deep learning results. In *Adv. Neural Inf. Process. Syst.*, 2017.
- Gemini Team, Rohan Anil, Sebastian Borgeaud, Jean-Baptiste Alayrac, Jiahui Yu, Radu Soricut, Johan Schalkwyk, Andrew M Dai, Anja Hauth, Katie Millican, et al. Gemini: a family of highly capable multimodal models. *arXiv preprint arXiv:2312.11805*, 2023.
- Zeyu Wang, Jingyu Lin, Yifei Qian, Yi Huang, Shichen Tian, Bosong Chai, Juncan Deng, Lan Du, Cunjian Chen, Yufei Guo, et al. Diffx: Guide your layout to cross-modal generative modeling. *arXiv preprint arXiv:2407.15488*, 2024.
- Yuxiang Wei, Yabo Zhang, Zhilong Ji, Jinfeng Bai, Lei Zhang, and Wangmeng Zuo. Elite: Encoding visual concepts into textual embeddings for customized text-to-image generation. In *Int. Conf. Comput. Vis.*, pages 15943–15953, 2023.
- Haoning Wu, Zicheng Zhang, Weixia Zhang, Chaofeng Chen, Liang Liao, Chunyi Li, Yixuan Gao, Annan Wang, Erli Zhang, Wenxiu Sun, et al. Q-align: Teaching llms for visual scoring via discrete text-defined levels. *arXiv preprint arXiv:2312.17090*, 2023.
- Guangxuan Xiao, Tianwei Yin, William T. Freeman, Frédo Durand, and Song Han. Fastcomposer: Tuning-free multi-subject image generation with localized attention. *arXiv preprint arXiv:2305.10431*, 2023.
- Shaoan Xie, Zhifei Zhang, Zhe Lin, Tobias Hinz, and Kun Zhang. Smartbrush: Text and shape guided object inpainting with diffusion model. In *IEEE Conf. Comput. Vis. Pattern Recognit.*, pages 22428–22437, 2023.
- Shaoan Xie, Yang Zhao, Zhisheng Xiao, Kelvin CK Chan, Yandong Li, Yanwu Xu, Kun Zhang, and Tingbo Hou. Dreaminpainter: Text-guided subject-driven image inpainting with diffusion models. *arXiv preprint arXiv:2312.03771*, 2023.
- Peng Xing, Haofan Wang, Yanpeng Sun, Qixun Wang, Xu Bai, Hao Ai, Renyuan Huang, and Zechao Li. Csgo: Content-style composition in text-to-image generation. *arXiv preprint arXiv:2408.16766*, 2024.
- Tao Xu, Pengchuan Zhang, Qiuyuan Huang, Han Zhang, Zhe Gan, Xiaolei Huang, and Xiaodong He. Attngan: Fine-grained text to image generation with attentional generative adversarial networks. In *IEEE Conf. Comput. Vis. Pattern Recognit.*, pages 1316–1324, 2018.

- Jiale Xu, Weihao Cheng, Yiming Gao, Xintao Wang, Shenghua Gao, and Ying Shan. Instantmesh: Efficient 3d mesh generation from a single image with sparse-view large reconstruction models. *arXiv preprint arXiv:2404.07191*, 2024.
- Zeyue Xue, Guanglu Song, Qiushan Guo, Boxiao Liu, Zhuofan Zong, Yu Liu, and Ping Luo. Raphael: Text-to-image generation via large mixture of diffusion paths. In *Adv. Neural Inf. Process. Syst.*, 2024.
- Jiahui Yu, Yuanzhong Xu, Jing Yu Koh, Thang Luong, Gunjan Baid, Zirui Wang, Vijay Vasudevan, Alexander Ku, Yinfei Yang, Burcu Karagol Ayan, et al. Scaling autoregressive models for content-rich text-to-image generation. *arXiv preprint arXiv:2206.10789*, 2022.
- Lvmin Zhang, Anyi Rao, and Maneesh Agrawala. Adding conditional control to text-to-image diffusion models. In *Int. Conf. Comput. Vis.*, pages 3836–3847, 2023.
- Xulu Zhang, Xiao-Yong Wei, Wengyu Zhang, Jinlin Wu, Zhaoxiang Zhang, Zhen Lei, and Qing Li. A survey on personalized content synthesis with diffusion models. *arXiv preprint arXiv:2405.05538*, 2024.
- Yuxuan Zhang, Yiren Song, Jiaming Liu, Rui Wang, Jinpeng Yu, Hao Tang, Huaxia Li, Xu Tang, Yao Hu, Han Pan, et al. Ssr-encoder: Encoding selective subject representation for subject-driven generation. In *Proceedings of the IEEE/CVF Conference on Computer Vision and Pattern Recognition*, pages 8069–8078, 2024.
- Guangcong Zheng, Xianpan Zhou, Xuwei Li, Zhongang Qi, Ying Shan, and Xi Li. Layoutdiffusion: Controllable diffusion model for layout-to-image generation. In *IEEE Conf. Comput. Vis. Pattern Recognit.*, pages 22490–22499, 2023.

A More Details of Experimental Setup

A.1 Dataset

As there is no existing dataset specifically for component-controllable personalization, we curate a dataset from the internet to conduct experiments. Particularly, unlike previous works [Ruiz *et al.*, 2023; Kumari *et al.*, 2023] that focus on very few categories of concepts, the dataset contains concepts and components from various domains, such as characters, animation, buildings, objects, and animals. Overall, the dataset consists of 23 concept-component pairs totally with 138 reference images, where each concept/component contains 3 reference images and a corresponding category label. It is worth noting that the scale of this dataset is aligned with the scale of those datasets used in the compared methods [Gal *et al.*, 2022; Ruiz *et al.*, 2023; Kumari *et al.*, 2023; Avrahami *et al.*, 2023; Safaee *et al.*, 2024].

A.2 Implementation

We utilize SD 2.1 [Rombach *et al.*, 2022] as the pretrained T2I diffusion model. As commonly done, the resolution of reference images is set to 512×512 . Besides, the LoRA rank and alpha are set to 32. To simplify concept learning, we exclude the region of the target component from the segmentation masks of the target concept, *e.g.*, remove the hair from the person in a “<person> + <hair>” pair. For the warm-up and DS-Bal stage, we set the learning rate to $1e-4$ and $1e-5$ and the training steps to 200 and 300. Moreover, the learning rate is further scaled by the batch size, which is set to completely contain a concept-component pair. For the cross-attention loss, we follow [Avrahami *et al.*, 2023] to average the corresponding cross-attention maps at resolution 16×16 and normalized them to $[0, 1]$. The model is trained with an AdamW [Loshchilov and Hutter, 2017] optimizer and a DDPM [Ho *et al.*, 2020] sampler. As done in [Avrahami *et al.*, 2023], the tensor precision is set to float16 to accelerate training. For a fair comparison, all random seeds are fixed at 0, and all compared methods use the same implementation above except for method-specific configurations.

A.3 Evaluation

To generate images for evaluation, we carefully design 20 text prompts covering extensive situations, which are listed in Tab. 4. These text prompts can be divided into four aspects, including recontextualization, restylization, interaction, and property modification, where each aspect is composed of 5 text prompts. In recontextualization, we change the contexts to different locations and periods. In restylization, we transfer concepts into various artistic styles. In interaction, we explore the spatial interaction with other concepts. In property modification, we modify the properties of concepts in rendering, views, and materials. Such a group of diverse text prompts allows us to systemically evaluate the generalization capability of a method. We generate 32 images per text prompt for each pair, using a DDIM [Song *et al.*, 2020] sampler with 50 steps and a classifier-free guidance scale of 7.5. To ensure fairness, we fix the random seed within the range of $[0, 31]$ across all methods. This process results in 14,720 images for each method to be evaluated, ensuring a thorough comparison.

A.4 Automatic Metrics

We utilize four automatic metrics in the aspects of text alignment (CLIP-T [Gal *et al.*, 2022]) and identity fidelity (CLIP-I [Radford *et al.*, 2021], DINO [Oquab *et al.*, 2023], DreamSim [Fu *et al.*, 2023]). To precisely measure identity fidelity, we improve the traditional measurement approach for personalization. This is because a reference image of the target concept/component could contain an undesired component/concept that is not expected to appear in evaluation images. Specifically, we use Grounded-SAM [Ren *et al.*, 2024] to segment out the concept and component in each reference and evaluation image. Then, we further eliminate the target component from the segmented concept as we have done during training. Such a process is similar to the one adopted in [Avrahami *et al.*, 2023]. As a result, using the segmented version of evaluation images and reference images, we can accurately calculate the metrics of identity fidelity.

A.5 User Study

We further evaluate the methods with a user study. Specifically, we design a questionnaire to display 20 groups of evaluation images generated by our method and other methods. Besides, each group also contains the corresponding text prompt and the reference images of the concept and component, where we adopt the same text prompts that are used to calculate CLIP-T. The results of our method and all the compared methods are presented on the same page. Clear rules are established for users to evaluate in three aspects, including text alignment, identity fidelity, and generation quality. Users are requested to select the best result in each group by answering the corresponding questions of these three aspects. We hide all the method names and randomize the order of methods to ensure fairness. Finally, 3,180 valid answers are collected for a sufficient evaluation of human preferences.

A.6 Compared Methods

In our experiments, we compare MagicTailor with SOTA methods in the domain of personalization, including Textual Inversion (TI) [Gal *et al.*, 2022], DreamBooth-LoRA (DB) [Ruiz *et al.*, 2023], Custom Diffusion (CD) [Kumari *et al.*, 2023], Break-A-Scene (BAS) [Avrahami *et al.*, 2023], and CLiC [Safaee *et al.*, 2024]. We select these methods because TI, DB, and CD are three representatives of personalization frameworks and BAS and CLiC are highly relevant to learning fine-grained elements from reference images. For TI, DB, and CD, we use the third-party implementation in Diffusers [Face, 2022]. For BAS, we use the official implementation. For CLiC, we reproduce it following the resource paper as the official code is not released. Unless otherwise specified, method-specific configurations are set up by following their resource papers or Diffusers. We empirically adjust the learning rate of CD and CLiC to $1e-4$ and $5e-5$ respectively, because they perform very poorly with the original learning rates. For a fair and meaningful comparison, these methods should be adapted to our task setting with minimal modification. Therefore, for those methods adopting a vanilla diffusion loss, we integrate the masked diffusion loss into them while using the same segmentation masks from MagicTailor.

Table 4: **Text prompts used to generate evaluation images.** These text prompts can be divided into four aspects: recontextualization, restylization, interaction, and property modification, covering extensive situations to systemically evaluate the method’s generalizability. Note that “<placeholder>” will be replaced by the combination of pseudo-words (e.g., “<tower> with <roof>”) when generating evaluation images, and will be replaced by the combination of category labels (e.g., “tower with roof”) when calculating the metric of text alignment.

Recontextualization	Restylization
“<placeholder>, on the beach”	“<placeholder>, watercolor painting”
“<placeholder>, in the jungle”	“<placeholder>, Ukiyo-e painting”
“<placeholder>, in the snow”	“<placeholder>, in Pixel Art style”
“<placeholder>, at night”	“<placeholder>, in Von Gogh style”
“<placeholder>, in autumn”	“<placeholder>, in a comic book”
Interaction	Property Modification
“<placeholder>, with clouds in the background”	“<placeholder>, from 3D rendering”
“<placeholder>, with flowers in the background”	“<placeholder>, in a far view”
“<placeholder>, near the Eiffel Tower”	“<placeholder>, in a close view”
“<placeholder>, on top of water”	“<placeholder>, made of clay”
“<placeholder>, in front of the Mount Fuji”	“<placeholder>, made of plastic”

B Additional Comparisons

B.1 Detailed Text-Guided Generation

One might wonder if component-controllable personalization can be accomplished by providing detailed textual descriptions to the T2I model. To investigate this, we separately feed the reference images of the concept and component into GPT-4o [Hurst *et al.*, 2024] to obtain detailed textual descriptions for them. The text prompt we used is “Please detailedly describe the <concept/component> of the upload images in a paragraph”, where “<concept/component>” is replaced with the category label of the concept or component. Then, we ask GPT-4o to merge these textual descriptions using natural language, and input them into the Stable Diffusion 2.1 [Rombach *et al.*, 2022] to generate the corresponding images. Some examples for a qualitative comparison are shown in Fig. 13. As we can see, such an approach cannot achieve satisfactory results, because it is hard to guarantee that visual semantics can be completely expressed by using the combination of text tokens. In contrast, our MagicTailor is able to accurately learn the desired visual semantics of the concept and component from reference images, and thus lead to consistent and excellent generation in this tough task.

B.2 Commercial Models

It is also worth exploring whether existing commercial models, which can understand and somehow generate both text and images by themselves or other integrated tools, are capable of handling component-controllable personalization. We choose two widely recognized commercial models, GPT-4o [Hurst *et al.*, 2024] and Gemini 1.5 Flash [Team *et al.*, 2023], for a qualitative comparison. First, we separately feed the reference images of the concept and component into them, along with the text prompt of “The uploaded images contain a special instance of the <concept/component>, please mark it as #<concept/component>”, where “<concept/component>” is replaced with the category label of the concept or component. Then, we instruct them to perform image generation, using the text prompt of “Please generate images containing #<concept> with #<component>”, where

“<concept>” and “<component>” are replaced with the category label of the concept and component, respectively. As shown in Fig. 14, these models struggle to reproduce the given concept, let alone reconfigure the concept’s component. Whereas, our MagicTailor achieves superior results in component-controllable personalization, using a dedicated framework designed for this task. It demonstrates that, even though large commercial models are able to tackle multiple general tasks, there is also plenty of room for the community to explore specialized tasks for real-world applications.

C More Ablation Studies and Analysis

C.1 Dynamic Intensity Matters

In Tab. 5, we explore DM-Deg by comparing it with 1) mask-out strategy; 2) fixed intensity; 3) linear intensity (α goes from 1 to 0, or from 0 to 1); and 4) dynamic intensity with different γ . First, the terrible performance of the mask-out strategy verifies that it is not a valid solution for semantic pollution. Notably, the descent linear intensity shows better identity fidelity than its ascent counterpart, which aligns with and validates our observations on noise memorization. Moreover, the dynamic intensity generally shows better results, and it can achieve better overall performance with a proper γ .

C.2 Momentum Denoising U-Net as a Good Regularizer

In Tab. 6, we study DS-Bal by modifying the U-Net for regularization as 1) fixed U-Net with $\beta = 0$ (i.e., the one just after warm-up); 2) fixed U-Net with $\beta = 1$ (i.e., the one from the last step); and 3) momentum U-Net with other β . The results show that employing the U-Net with a high momentum rate can yield better regularization to tackle semantic imbalance, thus leading to excellent performance.

C.3 Necessity of Warm-Up Training

In MagicTailor, we start with a warm-up phase for the T2I model to preliminarily inject the knowledge for the subsequent phase of DS-Bal. Here we investigate the necessity of

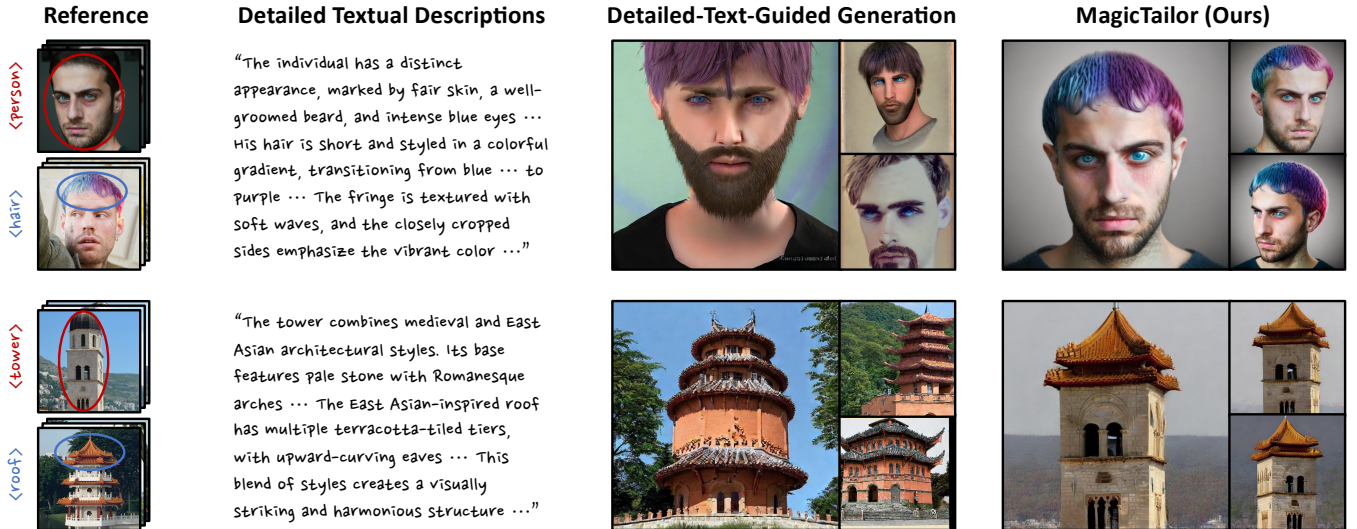


Figure 13: **Comparing with detailed-text-guided generation.** We use GPT-4o to generate and merge detailed textual descriptions for the target concept and component, which are fed into Stable Diffusion 2.1 to conduct text-to-image generation. This paradigm cannot perform well and produce inconsistent images, while MagicTailor can achieve faithful and consistent generation.

Table 5: **Ablation of DM-Deg.** We compare DM-Deg with its variants and the mask-out strategy. Our DM-Deg attains superior overall performance on text alignment and identity fidelity.

Intensity Variants	CLIP-T \uparrow	CLIP-I \uparrow	DINO \uparrow	DreamSim \downarrow
Mask-Out Strategy	0.270	0.818	0.760	0.375
Fixed ($\alpha = 0.4$)	0.270	0.849	0.800	0.297
Fixed ($\alpha = 0.6$)	0.271	0.845	0.794	0.310
Fixed ($\alpha = 0.8$)	0.271	0.846	0.796	0.305
Linear (Ascent)	0.270	0.846	0.797	0.307
Linear (Descent)	0.261	0.851	0.802	0.300
Dynamic ($\gamma = 8$)	0.266	0.850	0.806	0.289
Dynamic ($\gamma = 16$)	0.268	0.854	0.813	0.282
Dynamic ($\gamma = 64$)	0.271	0.852	0.812	0.283
Dynamic (Ours)	0.270	0.854	0.813	0.279

such a warm-up phase for generation performance. In Tab. 7, when removing the warm-up phase, even though MagicTailor could obtain slight improvement in text alignment, it severely suffers from the huge drop in identity fidelity. This is because such a scheme makes it difficult to construct a decent momentum denoising U-Net for DS-Bal. Whereas integrated with a warm-up phase, MagicTailor can achieve superior overall performance due to the knowledge reserved from warm-up.

C.4 Effectiveness of DM-Deg over Using Informative Training Prompts

One might be curious about whether it is not necessary to employ the proposed DM-Deg, but perhaps to use informative text prompts during training to provide textual prior knowledge for learning the target concept and component. To investigate this, we use Selectively Informative Description (SID) [Kim *et al.*, 2024] with GPT-4o [Hurst *et al.*, 2024] to construct text prompts for the target concept and component, and then use them for training. As shown in Fig. 15, such an

Table 6: **Ablation of DS-Bal.** We compare DS-Bal with potential variants, showing its excellence.

U-Net Variants	CLIP-T \uparrow	CLIP-I \uparrow	DINO \uparrow	DreamSim \downarrow
Fixed ($\beta = 0$)	0.268	0.850	0.803	0.293
Fixed ($\beta = 1$)	0.270	0.851	0.808	0.286
Momentum ($\beta = 0.5$)	0.268	0.850	0.805	0.290
Momentum ($\beta = 0.9$)	0.269	0.850	0.808	0.288
Momentum (Ours)	0.270	0.854	0.813	0.279

Table 7: **Ablations of warm-up.** We compare MagicTailor with the variant that removes warm-up. The results exhibit the significance of the warm-up stage for the framework of MagicTailor.

Warm-Up Variants	CLIP-T \uparrow	CLIP-I \uparrow	DINO \uparrow	DreamSim \downarrow
w/o Warm-Up	0.272	0.844	0.793	0.320
w/ Warm-Up (Ours)	0.270	0.854	0.813	0.279

approach cannot address semantic pollution well, where unwanted visual semantics still affect the personalized concept. In contrast, DM-Deg effectively prevents semantic pollution by dynamically perturbing those undesired visual semantics, verifying its remarkable significance in this task.

C.5 Robustness on Linking Words

Generally, we use “with” to link the pseudo-words of the concept and component in a text prompt, *e.g.*, “<person> with <beard>, in Von Gogh style”. Here we evaluate the robustness of our method on different linking words. We choose several words, which are commonly used to indicate ownership or association, to construct text prompts and then feed them into the same fine-tuned T2I model. As shown in Fig. 16, the generation performance of our MagicTailor remains robust regardless of the linking word used, exhibiting its flexibility to textual descriptions.

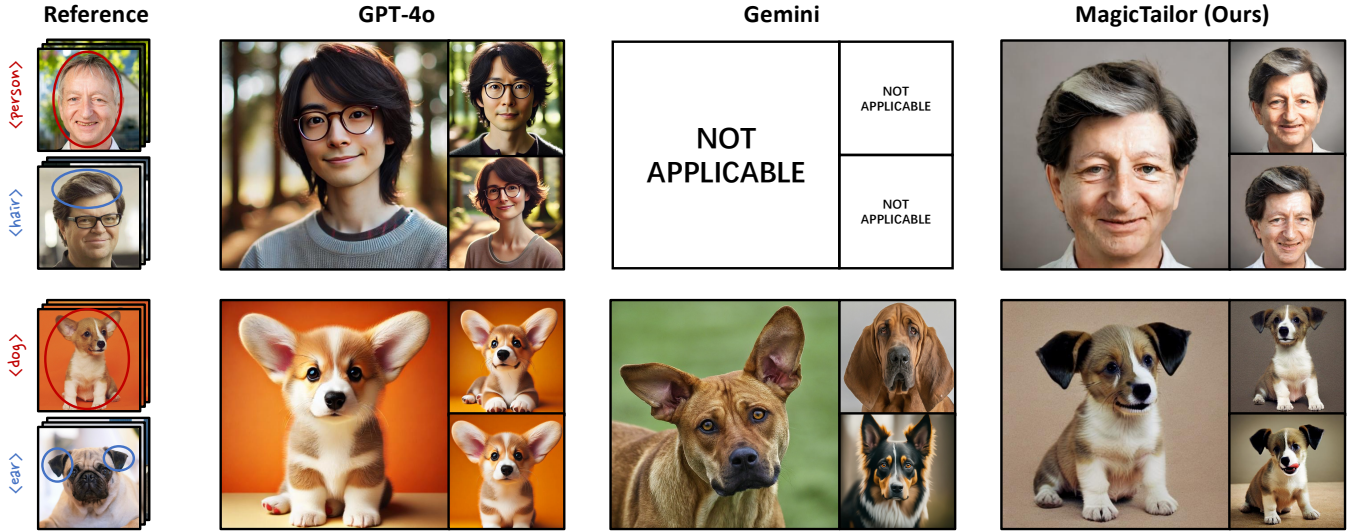


Figure 14: **Comparing with commercial models.** We input the reference images of the target concept and component to GPT-4o and Gemini, along with structured text prompts, for conducting image generation. Even though capable of handling multiple general tasks, these models still fall short in this task. In contrast, our MagicTailor performs well using a dedicated framework.

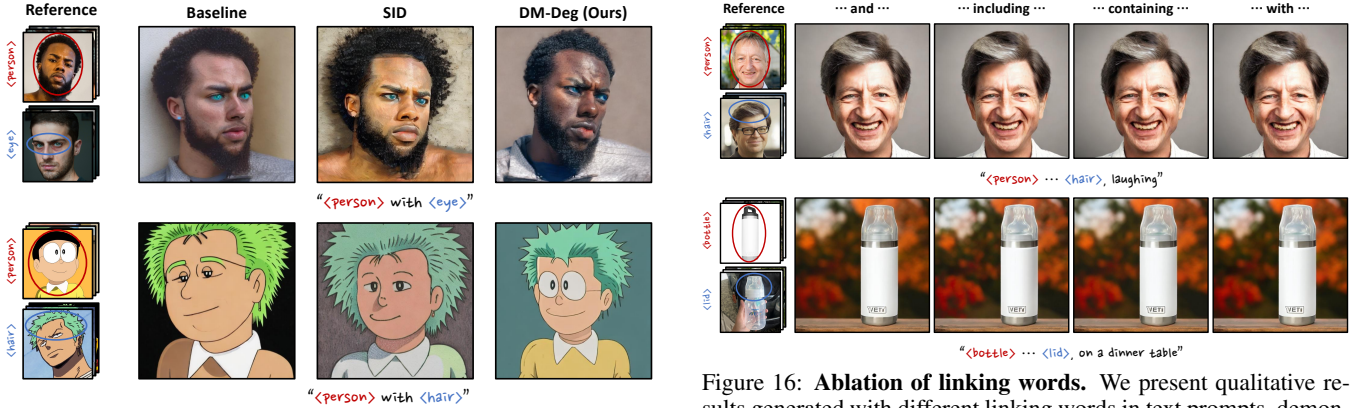


Figure 15: **Ablation of DM-Deg via replacement with SID.** We compare our DM-Deg with SID [Kim *et al.*, 2024] that aims to produce informative prompts for training. Besides, we also present baseline (*i.e.*, removing DM-Deg from MagicTailor) results for reference. This comparison indicates the effectiveness of our DM-Deg in addressing semantic pollution.

D More Qualitative Results

In Fig. 17 & Fig. 18, we provide more evaluation images for a substantial qualitative comparison. It can be clearly observed that semantic pollution remains an intractable problem for these compared methods. This is due to the leak of an effective mechanism to alleviate the T2I model’s perception for these semantics. To address this, our MagicTailor utilizes DM-Deg to dynamically perturb undesired visual semantics during the learning phase, and thus achieve better performance. On the other hand, the compared methods are also severely influenced by semantic imbalance, resulting in overemphasis or even overfitting on the concept or component. This is because the inherent imbalance of visual semantics complicates the learning process. In response to this issue, our MagicTailor applies DS-Bal to balance the learning of visual semantics, effectively showcasing its prowess in

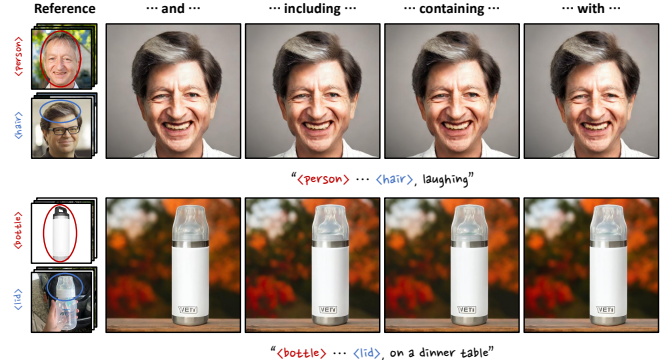


Figure 16: **Ablation of linking words.** We present qualitative results generated with different linking words in text prompts, demonstrating the robustness of MagicTailor.

this tough task. In summary, the proposed MagicTailor effectively addresses both semantic pollution and semantic imbalance through its innovative techniques, DM-Deg and DS-Bal, respectively. These advancements demonstrate its superiority in handling complex visual semantics and achieving remarkable performance in this challenging task.

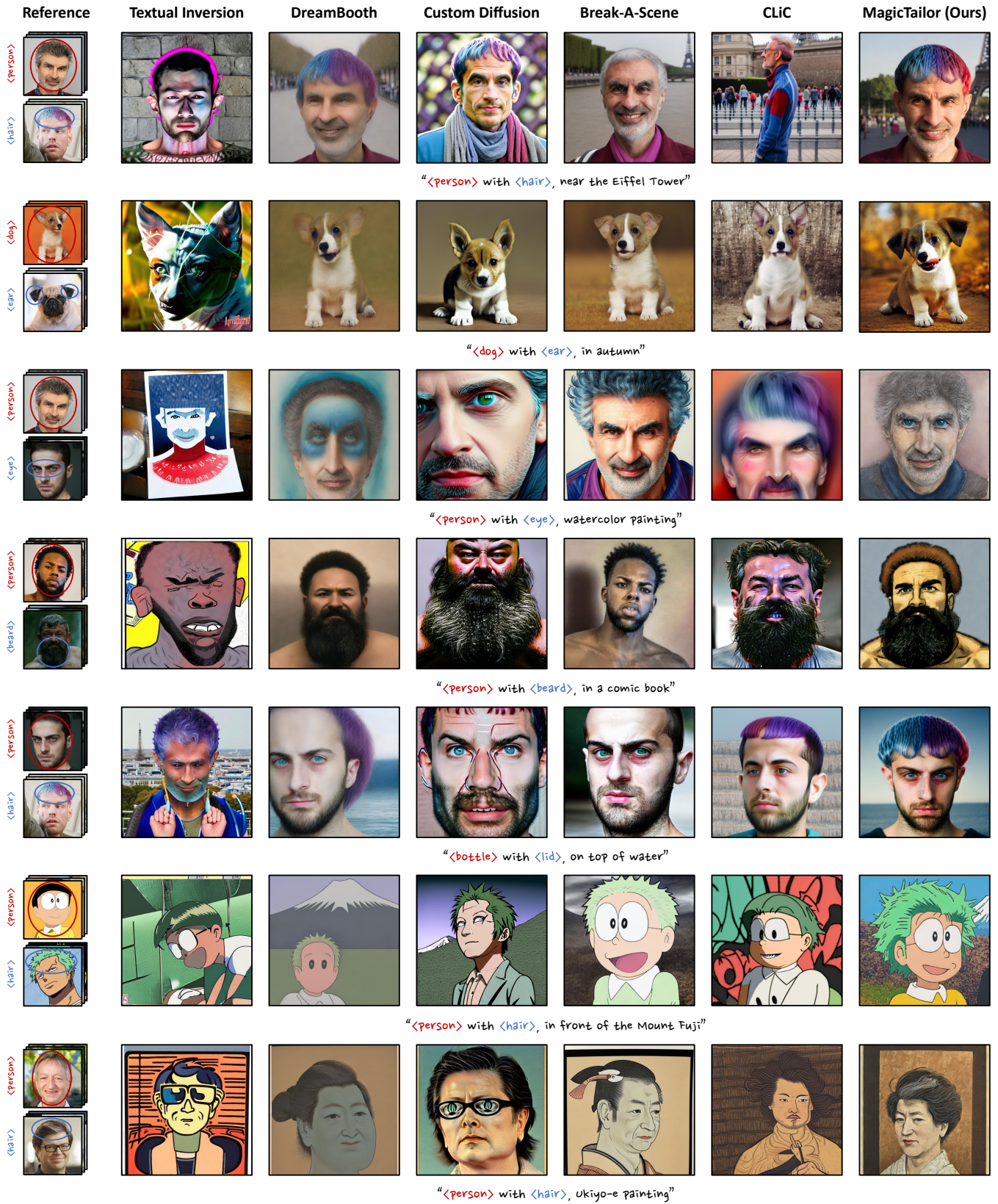


Figure 17: **More qualitative comparisons.** We present images generated by our MagicTailor and SOTA methods of personalization for various domains including characters, animation, buildings, objects, and animals. MagicTailor generally achieves promising text alignment, strong identity fidelity, and high generation quality.

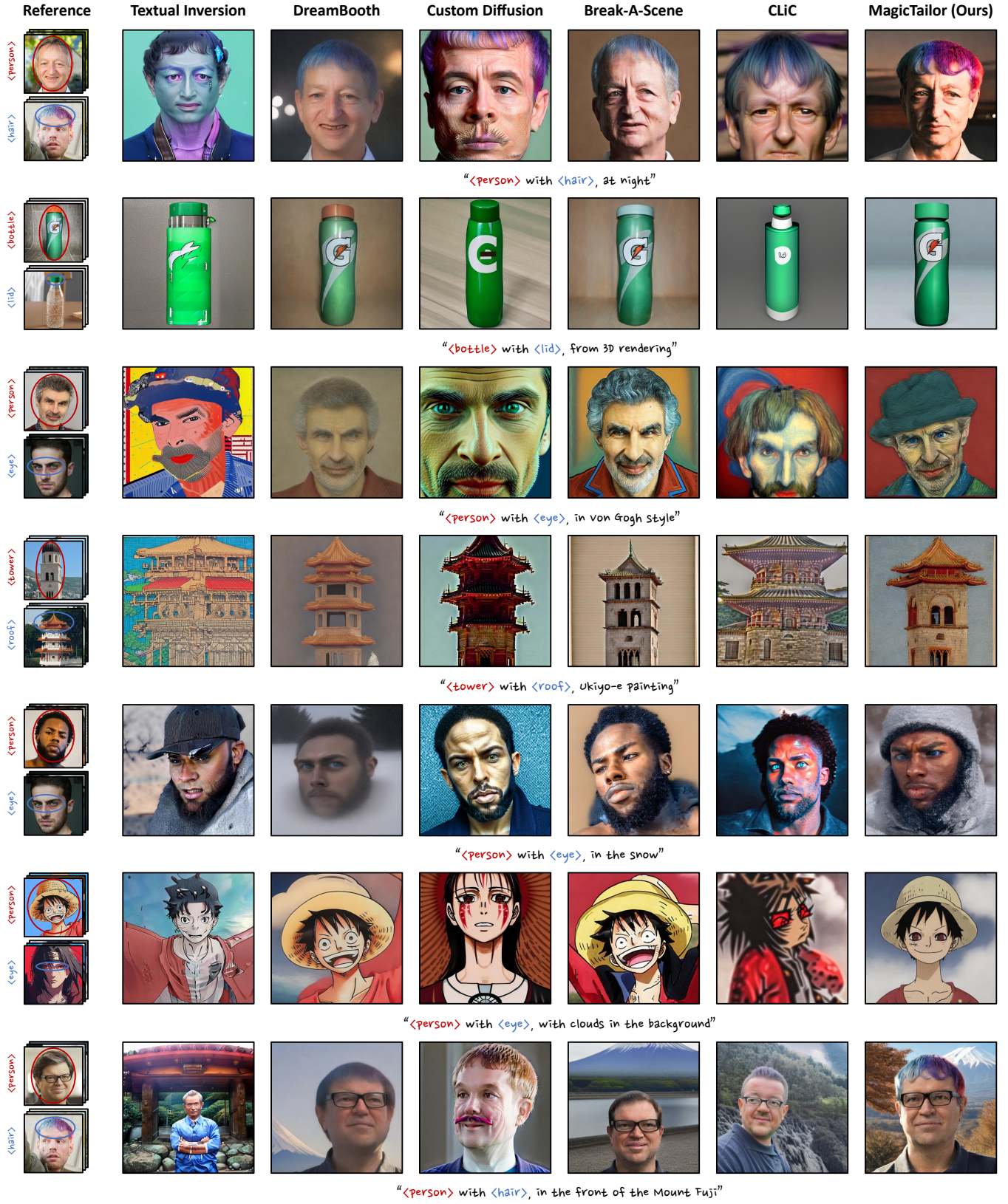


Figure 18: **More qualitative comparisons.** We present images generated by our MagicTailor and SOTA methods of personalization for various domains including characters, animation, buildings, objects, and animals. MagicTailor generally achieves promising text alignment, strong identity fidelity, and high generation quality.